Polymer Testing 30 (2011) 101–109

Contents lists available at ScienceDirect

Polymer Testing

journal homepage: www.elsevier.com/locate/polytest

Test Method

Characterization of viscoelastic-plastic properties of solid polymers by instrumented indentation

Jaroslav Menčík [a,*], Li Hong He [b], Jiří Němeček [c]

[a] University of Pardubice, Jan Perner Transport Faculty, 53210 Pardubice, Czech Republic
[b] University of Otago, Faculty of Dentistry, Dunedin 9054, New Zealand
[c] Czech Technical University, Faculty of Civil Engineering, 16629 Prague, Czech Republic

ARTICLE INFO

Article history:
Received 29 September 2010
Accepted 11 November 2010

Keywords:
Viscoelasticity
Elastic modulus
Hardness
Nanoindentation
Creep compliance function
PMMA

ABSTRACT

This paper presents formulae for visco-elastic-plastic response to indentation for various indenter shapes and times of loading, and describes a procedure for obtaining parameters of creep compliance function from monotonic load. The application is illustrated on PMMA, whose properties are measured under constant load and in a load-unload test. A discussion follows on the influence of indenter shape, various forms of creep compliance function and the relation between the test duration and the model. Also, other information obtainable from nanoindentation tests is mentioned: apparent modulus, hardness and components of creep compliance function.

1. Introduction

Instrumented indentation, also called nanoindentation, provides information about mechanical properties from indenter load and displacement measured continuously during loading and unloading. The advantages are a very small loaded volume, negligible damage and no special demands on test specimens except small size and smooth surface. Indentation methods are well developed for the determination of elastic modulus and hardness in elastic-plastic materials [1–3]. They are also suitable for testing of polymers and other materials with deformation depending not only on the load magnitude, but also on its duration (Fig. 1). In this case, the devices for instrumented indentation can provide the parameters of creep function from the load and displacement data recorded as functions of time.

The first papers about characterization of viscoelastic properties by nanoindentation appeared in the nineties, e.g. [4–7]. Very simple models were followed by more complex models and procedures [8–24], based on the theory of viscoelasticity [25–27]. Useful insight has also been obtained by finite element modeling [28]. The solid theoretical base, on the other hand, has enabled a unified approach and simple notation, suitable for practical use [15,16,20]. This will also be used in this paper, the aim of which is to provide general information on indentation testing of viscoelastic-plastic materials under monotonic load. (For testing under harmonic load see [29–31].)

The next section presents the main formulae. Then, a procedure is described for obtaining parameters of creep compliance function. Practical application is illustrated on polymethyl-methacrylate. The following discussion on the general properties of creep functions can help in the choice of test conditions and a suitable model. The last part of the paper shows some additional information obtainable from nanoindentation tests.

2. Theory

In elastic-plastic materials, such as metals or ceramics, low stresses cause only elastic deformations, which disappear after unloading. Stresses exceeding the material's

* Corresponding author.
E-mail address: jaroslav.mencik@upce.cz (J. Menčík).

0142-9418/$ – see front matter © 2010 Elsevier Ltd. All rights reserved.
doi:10.1016/j.polymertesting.2010.11.006

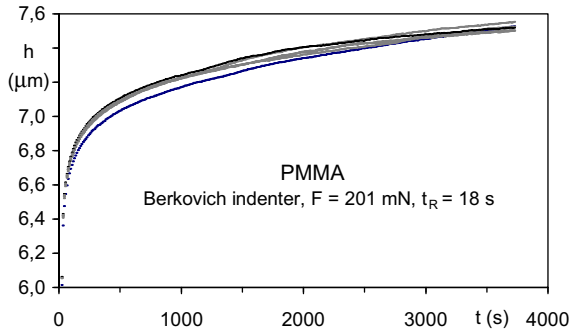

Fig. 1. Indenter penetration into PMMA under constant load during dwell II. Six tests. h – depth, t – time.

yield strength also cause plastic flow and permanent deformation. All these processes are usually considered as instantaneous.

The response of viscoelastic materials is more complex and depends on the stress level and the material's structure and bonds. In solid polymers, low stresses cause instantaneous elastic deformations and also delayed ones, which are reversible and disappear some time after unloading. In some materials, slow irreversible viscous flow also occurs. High stresses cause permanent changes in all viscoelastic-plastic solids, which can be either instantaneous (plastic) or time-dependent (viscous).

The load response can be described by various models, with parameters obtainable (also) from nanoindentation tests. When preparing these tests, one must know what information is needed. The stresses in many components are low, causing only reversible deformations. Thus, the stresses in the tests for study of this behavior should also be low. This can mean a limitation on the choice of indenter shape. There are three principal shapes: pointed, spherical, and cylindrical with flat end. Pointed indenters are very common, e.g. Vickers or Berkovich (Fig. 2), especially for the determination of hardness and elastic modulus. However, the stress concentration under these indenters is very high and usually leads to permanent deformation. With spherical indenters, the contact stresses are low for low loads and large indenter radii, and gradually grow with increasing load. If this load exceeds some value, irreversible deformation occurs as well.

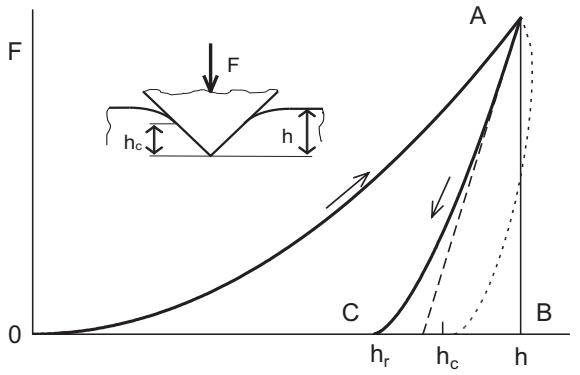

Fig. 2. Load–depth curves of an indentation test (a schematic). F – load, h – total depth of penetration, h_c – contact depth, h_r – residual depth after unloading. Dotted curve at the right – unloading curve typical of viscoelastic materials.

2.1. Formulae for indentation testing of elastic-plastic materials

The principal characteristics in nanoindentation tests, hardness H and elastic modulus E, are determined from a load-unload cycle (Fig. 2). Hardness is defined as the mean contact pressure under the loaded indenter:

$$H = p_m = \frac{F}{A} \tag{1}$$

F is the load and A is the projected contact area, determined from the contact depth h_c, calculated from the total penetration h, indenter load and contact stiffness $S\,(=\mathrm{d}F/\mathrm{d}h)$ at the beginning of unloading (Fig. 2). Most often, the formula by Oliver and Pharr [1] is used:

$$h_c = h - \varepsilon\frac{F}{S} \tag{2}$$

where ϵ is a constant ($\epsilon = 0.75$ for a spherical or pointed indenter, and $\epsilon = 0$ for a flat punch). The stiffness S is determined from the unloading curve fitted by a regression function [1]:

$$F = k(h - h_p)^m \tag{3}$$

with empirical constants k, h_p and m. Contact area for a Berkovich or Vickers indenter is $A \approx 24.5\ h_c^2$; for a spherical indenter of tip radius R and small depth of penetration, $A = 2\pi R h_c$. The contact area and stiffness also serve for the determination of the reduced modulus E_r:

$$E_r = \frac{\sqrt{\pi}}{2\beta}\frac{S}{\sqrt{A}} \tag{4}$$

β is the correction factor for indenter shape ($\beta = 1$ for circular contact and 1.05 for Berkovich indenter). E_r is related to the elastic (Youngs) modulus E and Poisson's ratio ν of the sample (no subscript) and indenter (subscript i) as

$$1/E_r = (1-\nu^2)/E + (1-\nu_i^2)/E_i \tag{5}$$

Equation (4) is valid for elastic as well as elastic-plastic indentation and for any indenter of axisymmetrical shape. For purely elastic contact with a spherical indenter, Hertz' formulae may also be used:

$$h = \sqrt[3]{\frac{9F^2}{16RE_r^2}} \tag{6}$$

$$p_m = \frac{1}{\pi}\sqrt[3]{\frac{6FE_r^2}{R^2}} \tag{7}$$

The elastic modulus can be obtained from the load and displacement using the rearranged Eq. (6), or by fitting several points $h(F)$ by Eq. (6). Contact depth is related to the total depth of elastic penetration as $h_c = h/2$.

2.2. Theoretical background for characterization of viscoelastic properties by indentation

The load response of solid polymers depends on the load magnitude and duration. Deformation grows even under constant load (Fig. 1), and after unloading it gradually diminishes. The mean contact pressure decreases with the time under load.

If the deformation is only reversible and small, it can be calculated using the elastic solution with the apparent modulus $E(t)$ or creep compliance function $J(t)$ corresponding to the time t under load. There are two limit cases: very short duration of loading and very long time under load, with the "instantaneous" modulus $E_0(t \to 0)$ and asymptotic value $E_\infty(t \to \infty)$, respectively. The time course of $J(t)$ or $E(t)$ can be determined, e.g., by indentation.

In load-unload nanoindentation tests, common for the determination of elastic modulus and hardness, a role is played by the velocity of load increase and the time under load. Also, due to delayed response, the unloading part of the F–h curve is often distorted – more convex than for elastic materials (dotted curve in Fig. 2). As a consequence, the apparent contact stiffness S, determined from the unloading curve as $(\mathrm{d}F/\mathrm{d}h)_{\mathrm{Fmax}}$, is higher than the actual value. This can lead to an error in the determination of contact depth and area, as well as of the elastic modulus and hardness [28,32–34].

The influence of viscoelastic after-effects can be reduced in various ways. Often, a dwell time is inserted between the loading and unloading. Cheng and Cheng [28] recommend very quick unloading. According to Chudoba and Richter [33], the effect of delayed deforming on the unloading curve may be neglected if the penetration depth grows less than 1% per minute. It is also reduced if the contact depth is calculated using the effective contact stiffness S, proposed by Feng and Ngan [34]:

$$\frac{1}{S} = \frac{1}{S_{app}} + \frac{\dot{h}_d}{|\dot{F}_u|} \tag{8}$$

S_{app} is the apparent stiffness, obtained from the unloading curve by the common Oliver & Pharr procedure; $\dot{h}_d$ is the indenter velocity ($\mathrm{d}h/\mathrm{d}t$) at the end of dwell, and $\dot{F}_u$ is the load decrease rate $\mathrm{d}F/\mathrm{d}t$ at the beginning of unloading.

A disadvantage of this approach is that the indenter depth h at the beginning of unloading is larger than at the end of load increase. This results in larger contact area and lower apparent hardness. Moreover, it is generally insufficient to characterize materials which flow under load only by a single value of hardness or elastic modulus. The time-dependent properties are described better by rheological (spring-and-dashpot) models, which are universal and their parameters may be used in commercial software for finite element analysis. These parameters can be obtained by fitting the time course of indenter penetration by a suitable creep function.

The pertinent formulae are based on the approach proposed by Lee and Radok [25,26]. This approach uses the elastic solution, but replaces the elastic constants by a viscoelastic integral operator. The relationship between the indenter load F and depth h of penetration under monotonic load can be expressed as

$$h^m(t) = K\,\psi(F,J,t) \tag{9}$$

m and K are constants for the indenter geometry, and $\psi(F,J,t)$ is a response function depending on the load, material parameters and time. For pointed indenters (cone, Berkovich or Vickers), $m = 2$ and $K = \pi/(2\tan\alpha)$; α is the semi-angle of indenter tip or of equivalent cone; for Berkovich and Vickers, $\alpha = 70.3°$. For a spherical indenter, $m = 3/2$ and $K = 3/(4\sqrt{R})$, where R is the tip radius.

The general form of response function for linearly viscoelastic materials is [27]:

$$\psi(t) = \int_0^t J(t-u)[dF/du]du \tag{10}$$

$J(t)$ is the creep compliance function – a basic material characteristic expressing the time course of its response to a step unit load; t is time, and u is a dummy variable for integration. For constant load after step change from 0 to F,

$$\psi(t) = FJ(t) \tag{11}$$

However, there is always some period of load increase. Fortunately, there are two load regimes, leading to simple response functions. If the load grows by a constant rate $k = \mathrm{d}F/\mathrm{d}t = const$,

$$\psi(t) = k\int_0^t J(t-u)du \tag{12}$$

In this case, the test duration is limited by attaining the maximum possible force F. For longer times, a two-step arrangement is better. The load first grows by a constant rate k to the nominal value F, and then it is held constant. For this second period, Eq. (12) can be used, with the upper integration limit t equal to the duration of load increase, $t_{\mathrm{R}}\,(= F/k)$.

2.3. Creep compliance and response functions

2.3.1. Reversible viscoelastic deformation

A universal model consists of a spring in series with one or more Kelvin-Voigt bodies (a spring in parallel with a dashpot). The creep compliance function for the model with n Kelvin-Voigt bodies is

$$J(t) = C_0 + \sum_{j=1}^{n} C_j\left[1 - \exp\left(-t/\tau_j\right)\right] \tag{13}$$

C_0 and C_{j} are compliance constants, and τ_{j} is time constant (retardation time), related to the compliance C_{j} of the spring and dynamic viscosity η_{j} of the dashpot in the j-th Kelvin-Voigt body as $\tau_{\mathrm{j}} = \eta_{\mathrm{j}}C_{\mathrm{j}}$. Creep compliance function is related to the apparent reduced modulus as

$$J(t) = 1/E_r(t) \tag{14}$$

Its time-independent part, C_0, corresponds to the reciprocal of reduced elastic modulus, $1/E_{\mathrm{r},0}$. With a stiff indenter,

$$C_0 = \left(1-\nu^2\right)/E_0 \tag{15}$$

Equation (13) can also be written in the form of a Prony

series, used in computer codes for finite element analysis of viscoelastic and creep problems:

$$J(t) = B_0 - \sum C_j \exp(-t/\tau_j),\ j = 1, 2 \ldots n \quad (16)$$

where $B_0 = C_0 + \sum C_j$

Indentation creep under constant load F after step change at $t = 0$ is described by Eq. (11) with the creep compliance function (13). If the load first increases from zero with constant rate k and, after reaching the nominal value F is kept constant, the combination of Eqs. (12) and (13) gives for $t \geq t_R$:

$$\psi(t) = F\left\{C_0 + \sum C_j\left[1 - \rho_j \exp(-t/\tau_j)\right]\right\} \quad (17)$$

where ρ_j is a ramp correction factor, as introduced by Oyen [16]:

$$\rho_j = (\tau_j/t_R)\left[\exp(t_R/\tau_j) - 1\right] \quad (18)$$

For loading with short load increase compared to the retardation times, $t_R \ll \tau_j$, the ramp correction factor ρ_j is close to 1; it attains 1.025 for $t_R/\tau_j = 0.05$ and 1.05 for $t_R/\tau_j = 0.1$, and grows rapidly for higher ratios of t_R/τ_j.

2.3.2. Viscoelastic-plastic response

In some cases, irreversible deformations also occur. They can be time-independent (plastic), or time-dependent (viscous). Plastic behavior can be characterized by a slider in the rheological model. Its characteristic (= yield strength Y or hardness H_0) is contained together with that for the instantaneous elastic response (E_0) in the compliance C_0. The time-dependent irreversible viscous deformation is characterized by a dashpot of viscosity η, arranged in series with the other bodies. The creep compliance function is

$$J(t) = C_0 + c_v t + \sum C_j\left[1 - \exp(-t/\tau_j)\right] \quad (19)$$

$c_v = 1/\eta$ is viscous compliance. The response function for indentation creep under constant force F after the load increase period t_R is

$$\psi(t) = F\left\{C_0 + c_v(t - tR/2) + \sum C_j\left[1 - \rho j \exp(-t/\tau_j)\right]\right\} \quad (20)$$

The term $-Ft_R/2$ reflects the fact that the viscous deformation during the load increase is proportional to the average force $F/2$. If no irreversible viscous flow occurs, $c_v = 0$.

3. Procedure for the determination of viscoelastic-plastic properties

The parameters in the creep compliance function may be obtained from the time course of indenter penetration under load. A universal five step procedure is shown in Fig. 3. In the first step (I) of duration t_R, the indenter is loaded at constant rate k to the nominal load F. A dwell time II under this load follows, then unloading III to a very low load F_u, followed by a dwell time IV and unloading to zero (V). The response during dwell II serves for the determination of viscoelastic parameters, while the back-creep during the low load dwell IV serves for revealing the irreversible components of deformation and check of the duration of reversible processes and the number of Kelvin-Voigt elements.

The loading in step I should be fast in order to reduce the time-dependent processes here. The dwell II under constant load should last so long that the duration of all reversible viscoelastic processes can be assessed. The unloading III should also be fast, and the constant load F_u in the following period IV should be very low, so that the indenter only remains in contact with the specimen and serves for monitoring of deformation recovery. The period IV should last about the same time as period II.

The constants in the creep compliance function are obtained from the dwell II. For the response function (19), equation (10) gives for $t \geq t_R$:

$$h^m(t) = FK\left\{C_0 + c_v(t - t_R/2) + \sum C_j\left[1 - \rho_j \exp(-t/\tau_j)\right]\right\} \quad (21)$$

F is the nominal load, and m, K are constants for the given indenter shape, as defined at Eq. (9). If no irreversible viscous flow occurs, all terms with c_v are left out. The constants C_0, c_v, C_1, τ_1, ρ_1, etc. can be obtained by minimizing the sum of squared differences between the measured and calculated $h^m(t)$ values. However, the actual procedure must be modified. Equation (21) contains several terms which do not depend on time: C_0, $c_v t_R/2$ and C_j, and regression analysis can determine them only as a whole. Moreover, the terms $C_j\rho_j$ are present, with the ramp correction factors ρ_j depending on the retardation times τ_j, which are as yet unknown. Actually, Eq. (21) corresponds to the series (16) extended by $c_v t$:

$$h^m(t) = FK\left[B_0 + c_v t - \sum D_j \exp(-t/\tau_j)\right] \quad (22)$$

with

$$B_0 = C_0 - c_v t_R/2 + \sum C_j,\ and\ D_j = C_j\rho_j;\ j = 1, 2, 3\ldots \quad (23)$$

The determination of model parameters proceeds in three steps:

Step 1. Calculation of regression constants B_0, c_v, D_j and retardation times τ_j in the proposed model by fitting the $h^m(t)$ data from period II (for $t \geq t_R$) by the function (22).

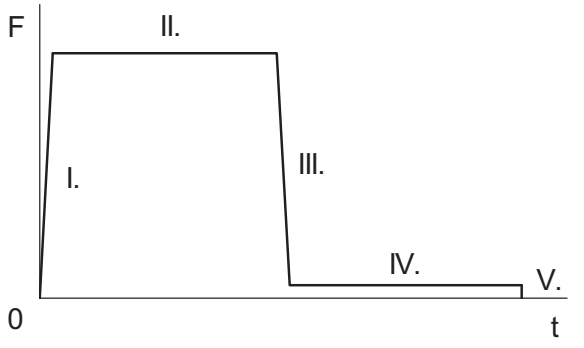

Fig. 3. Five-step procedure (I. – V.) for the determination of parameters in creep compliance function.

Step 2. Calculation of the ramp correction factors ρ_j from Eq. (18) for the known duration t_R of load increase and the retardation times τ_j. Then, the constants C_j are found as $C_j = D_j/\rho_j$.

Step 3. Determination of C_0 from Eq. (23) as

$$C_0 = B_0 + c_v t_R/2 - \sum C_j \quad (24)$$

Besides these measurements, tests with fast loading and unloading can also be done in order to obtain "instantaneous" elastic modulus and hardness; cf. Section 2.1.

4. Experimental part

The method for obtaining viscoelastic-plastic parameters was tested on polymethyl-methacrylate, epoxy resin and tooth enamel. In all tests, the character and quality of results was similar. Therefore, only the tests with PMMA (heat cured dental acrylic, manufacturer: Vertex-Dental B.V.) are described here; for tooth enamel, see [21]. A UMIS-2000 nanoindenter with diamond Berkovich indenter was used. Two groups of tests were done; one for obtaining viscoelastic parameters from the creep data, and the other for the determination of elastic modulus and hardness.

4.1. Creep tests

Six tests were made according to the five step loading scheme (Fig. 3). As the purpose of this study was to obtain a better idea about the possibilities of modeling the load response of viscoelastic solids, a long dwell under load was used and also several rheological models. The indenter load grew for 18 s to the nominal value $F = 201$ mN and then was held constant for 3700 s. Then, it was unloaded in 24 s to $F_u = 10$ mN, kept constant for 3630 s and then unloaded to zero. The characteristic depths grew under nominal load from 6.0 to 7.6 μm. During unloading to F_u they decreased quickly to 4.7 μm and then (during the following dwell) gradually to 3.5 μm. While the indenter penetrated into the specimen all the time under nominal load without signs of stopping, the back-creep after unloading to F_u ceased after about 1800 s. The differences between individual h–t curves were small (Fig. 1).

The load-displacement curve during dwell II was approximated by seven models described by Eq. (22): 1) S + KV, 2) S + 2 KV, 3) S + 3 KV, 4) S + 4 KV, 5) S + D + KV, 6) S + D + 2 KV, 7) S + D + 3 KV; S means spring, D dashpot, and K-V Kelvin-Voigt body. The constants B, c_v, D_j and τ_j in Eq. (22) were obtained by minimizing the sum of the squared differences between the quadrates of the measured and calculated depths, $\Sigma[h_m^2(t_j) - h_c^2(t_j)]^2$, using the solver in Excel. Then, the ramp correction factors ρ_j and constants C_0, C_j were found. The quality of fit was also illustrated by the relative differences between measured and calculated values, $\Delta_{rel,j} = [h_m(t_j) - h_c(t_j)]/h_m(t_j)$.

The results can be summarised as follows. The creep compliance function (21) with several exponential terms has proved very suitable for the characterization of long viscoelastic processes. Very good fits (relative errors not exceeding a few tenths of a percent anywhere) were obtained for models S + 4 KV, S + 3 KV, S + D + 3 KV and S + D + 2 KV. Good fits were also obtained with models S + D + KV and S + 2 KV; the errors made tenths of a percent for longer times and up to a few percent at the beginning of the test. With the simplest model, S + 1 KV, the differences between the measured and calculated values were obvious, with the maximum difference 11% for short times. Two examples (S + D + 2 KV and S + KV) are shown in Fig. 4. Tables 1 and 2 show the constants in creep compliance functions for two models with good fit (S + D + 2 KV and S + 3 KV). In models with two or more K-V bodies, similarly good fits were obtained regardless of whether or not a dashpot was used. However, the loaded indenter continued penetrating after 1 h without signs of stopping, but the back-creep essentially ceased after half an hour (Fig. 5). This indicates that high stresses beneath the sharp indenter tip promoted irreversible viscous flow, so that a dashpot in series with other elements is more appropriate in the model.

As obvious from the tables, the retardation times τ_j and constants C_j in various models were different; even the "instantaneous" compliance C_0 differed by up to 38%. Also, the constants in the same model varied significantly between individual indents. On the other hand, good fits were also obtained if fixed retardation times were chosen (about the averages of "free" values) and only the constants C_0, C_1, … were optimized. In this case, the sum of squared differences was somewhat higher, but the differences between constants in the individual tests were smaller. Despite significant differences between the fixed and "free" retardation times, the resultant creep compliance functions were close each other. Table 1 also shows the sums of squared differences between the measured and calculated values; the difference between both approaches is not large.

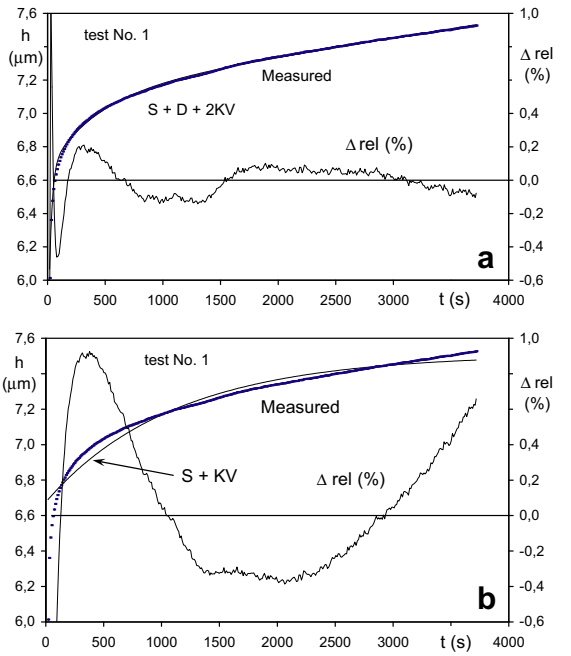

Fig. 4. Indenter penetration into PMMA under constant load. a) Model "S + D + 2 KV", b) model "S + KV". The model S + D + 2 KV overlaps very well with the measured data; the differences are visible only via relative residuals Δ_{rel} (zig-zag lines). h – depth, t – time.

Table 1
Creep compliance function for PMMA. Test parameters: Berkovich indenter, $F = 201$ mN, time under load: 3700 s. Model: Spring + Dashpot + 2 K-Voigt bodies. SSQ – sum of squared differences between the measured and calculated values.

Test No.	C_0 (m^2/N)	c_v (m^2/Ns)	C_1 (m^2/N)	C_2 (m^2/N)	τ_1 (s)	τ_2 (s)	SSQ
a) All constants were obtained by the least squares method.							
1	2.969E-10	1.482E-14	9.707E-11	5.316E-11	25.37	440.27	4.937E+00
2	3.103E-10	1.101E-14	9.558E-11	5.902E-11	32.90	643.75	7.721E+00
3	2.923E-10	1.337E-14	1.023E-10	5.792E-11	20.16	357.73	2.665E+00
4	3.075E-10	1.058E-14	9.736E-11	5.627E-11	29.79	545.86	9.503E+00
5	3.094E-10	8.011E-15	9.926E-11	6.294E-11	31.37	664.06	7.669E+00
6	3.054E-10	1.006E-14	1.001E-10	5.651E-11	28.82	539.54	8.441E+00
b) Retardation times τ_1, τ_2, τ_3 were chosen, the other constants were obtained by the least squares method.							
1	2.940E-10	1.408E-14	1.021E-10	5.322E-11	25.0	500.0	5.449E+00
2	2.992E-10	1.269E-14	1.008E-10	5.943E-11	25.0	500.0	8.737E+00
3	2.983E-10	1.174E-14	1.047E-10	5.446E-11	25.0	500.0	5.735E+00
4	2.992E-10	1.103E-14	1.029E-10	5.752E-11	25.0	500.0	9.704E+00
5	3.009E-10	1.015E-14	1.016E-10	6.211E-11	25.0	500.0	9.187E+00
6	2.985E-10	1.046E-14	1.047E-10	5.752E-11	25.0	500.0	8.593E+00

4.2. Elastic modulus and hardness

Elastic modulus E and hardness H were determined in eight standard "load-unload" tests according to Fig. 2 and Eqs. (1)–(4), with the stiffness correction (8). The load increase to the nominal load 300 mN lasted 23 s, the dwell under nominal load lasted 62 s, and the unloading lasted 20.6 s.

The scatter of all results was very small, below 1%. The average values were: $E = 3.66$ GPa (individual values varied between 3.62 and 3.67 GPa) and $H = 0.205$ GPa (0.203–0.207 GPa); the maximum depths h varied between 8.12 and 8.20 μm. The indentation modulus was close to the values obtained by the authors for commercial sheet PMMA in bending tests with fast loading (3.7–3.9 GPa at 0.45 s, decreasing to 3.0 GPa after 1000 s).

5. Discussion

The creep compliance function (19) was able to fit the experimental data very accurately, but differences existed between the constants obtained for various models. One must be aware that the parameters in a creep function have no exact physical meaning. They should be understood just as regression constants which depend on the material, indenter shape, rheological model and test duration. Thus, if a creep compliance function is to serve for response characterization of a polymeric material, it must be used as a whole, with clearly defined conditions of its validity (e.g. time interval). Any constant alone is not sufficient as a characteristic.

For elastic deformations, the modulus E_0 can be related to the instantaneous compliance C_0 by Eq. (15). Inserting the average indentation modulus 3.66 GPa and Poisson's ratio 0.35 gives $C_0 = 2.40 \times 10^{-10}$ m^2/N. This is less than the values of creep compliance function obtained by fitting the creep data ($3.0–3.6 \times 10^{-10}$ m^2/N). The higher compliance C_0 in the latter case was obviously due to the fact that the very high stresses under the Berkovich indenter also caused plastic deformation. (The relationship between C_0 and E_0 is discussed in [21].)

The test parameters, especially the duration and indenter shape, should be arranged with respect to the character of the tested material and its potential use. As shown by Oyen [15,16], the creep compliance function from tests with a pointed indenter is sometimes not interchangeable with that obtained by a spherical indenter, and vice versa. The stresses under a pointed indenter are very high and also cause irreversible plastic and viscous flow. However, many polymeric materials are exposed to low stresses. In such cases, tests with a spherical indenter are better. Equation (7) can help in finding a proper combination of tip radius and

Table 2
Creep compliance function for PMMA. Test parameters: Berkovich indenter, $F = 201$ mN, time under load: 3700 s. Model: Spring + 3 K-Voigt bodies.

Test No.	C_0 (m^2/N)	C_1 (m^2/N)	C_2 (m^2/N)	C_3 (m^2/N)	τ_1 (s)	τ_2 (s)	τ_3 (s)
a) All constants were obtained by the least squares method.							
1	3.755E-10	1.041 E-10	5.008 E-11	1.046 E-10	13.3	171.9	2944.4
2	3.574E-10	1.084E-10	5.140E-11	9.245E-11	10.8	127.2	1914.5
3	4.024E-10	1.044E-10	5.411E-11	1.172E-10	17.0	269.9	5514.4
4	3,448E-10	1,132E-10	5,250E-11	8,248E-11	10.6	137.0	1926.2
5	3,416E-10	1,140E-10	5,098E-11	8,130E-11	10.1	115.2	1514.5
6	3,438E-10	1,128E-10	5,151E-11	7,929E-11	11.2	137.7	1847.8
b) Retardation times τ_1, τ_2, τ_3 were chosen, the other constants were obtained by the least squares method.							
1	3,643E-10	1,104E-10	2,870E-11	9,245E-11	13.0	130.0	1800.0
2	3,672E-10	1,011E-10	4,686E-11	9,172E-11	13.0	130.0	1800.0
3	3,601E-10	9,977E-11	4,850E-11	8,300E-11	13.0	130.0	1800.0
4	3,595E-10	9,939E-11	4,972E-11	8,235E-11	13.0	130.0	1800.0
5	3,597E-10	9,864E-11	5,272E-11	8,150E-11	13.0	130.0	1800.0
6	3,557E-10	1,011E-10	5,067E-11	7,967E-11	13.0	130.0	1800.0

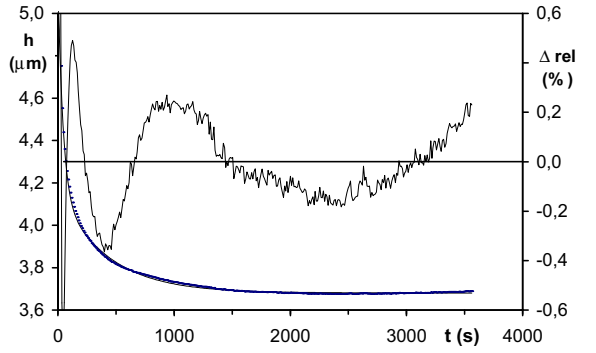

Fig. 5. Indenter displacement (backcreep) during dwell IV under low load. Measured and calculated values for the model "S + 2 KV", h – depth, t – time, Δ_{rel} – relative residuals.

load so that the contact pressure does not exceed the limit for plastic flow; this limit pressure is obtainable from tests with a pointed indenter and Eq. (1).

If a new material is investigated, it is important to ascertain the duration of reversible viscoelastic processes. A short test, lasting only tens of seconds, often gives incomplete information, and extrapolation of the corresponding creep compliance function $J(t)$ to long times can lead to significant errors (Fig. 6). The test duration should be similar to the duration of delayed reversible processes or of the load action in applications.

In a long term test, it is reasonable to fit the experimental $h(t)$ data by several creep compliance functions, and choose a model which fits the data well, but is not too complicated. The number of K-V elements depends, in general, on the duration of the investigated process. The response of a Kelvin-Voigt body, described by $C_j[1 - \exp(-t/\tau_j)]$, is active within about two orders of time; roughly for $0.03 < t/\tau_j < 3.0$. For example, $1 - \exp(-0.03) \approx 0.03$. Thus, for $t/\tau_j < 0.03$ the body hardly started reacting, and until this time it behaves as if it were stiff. On the other hand, $1 - \exp(-3) \approx 0.95$, so that for $t/\tau_j > 3$ nearly the full deformation has been reached, and the resultant response corresponds to a spring of compliance C_j alone. Therefore, longer processes need more K-V bodies in the model. Their suitable

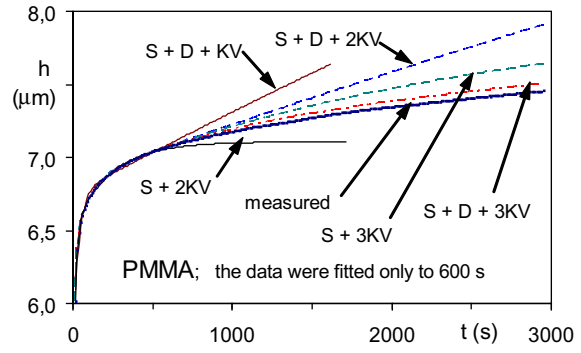

Fig. 6. Indenter penetration into PMMA – measured and calculated for various models (after [22]). The measurement lasted 3000 s, but only the first 600 s were used for the data fitting.

number can be checked from the back-creep during the low load dwell.

For models with only a few constants ($\leq$4), Solver easily finds the "best" parameters (C_0, C_1, τ_1…). With more constants, various "optimum" parameters are sometimes found for different starting values used in the search. The differences between $J(t)$ curves for individual fits are often negligible. Hence, it is possible to choose fixed retardation times τ_j reasonably scaled, for example $\tau_1 = 1$ s, $\tau_2 = 10$ s, $\tau_3 = 100$ s, etc. Solver then must seek only the constants C_0, C_1, etc., (which are only parameters in the model, valid for some time range.)

For polymers intended for long term loading, it is important to ascertain whether the indenter has stopped during the test or not. The former case can occur in tests with spherical indenters and low contact pressures, while continuting penetration is common with pointed indenters, with maximum contact stresses exceeding the limit for irreversible viscous flow. If the indenter has stopped, the number of K-V bodies should correspond roughly to the number of time orders of this process. For example, if $t_{stop} = 300$ s, two or three K-V bodies are sufficient and the model may also be used for longer times. If the indenter continues penetrating into the specimen at the end of test, the number of Kelvin-Voigt bodies should correspond to the test duration, and the model may be used only for processes not significantly longer than this time. Extrapolation can be dangerous; also the form of the creep compliance function $J(t)$ plays a role (Fig. 6). The test should, therefore, last as long as possible, a limitation sometimes being the time-stability of the indentation device.

The load increase at the beginning of the test should be fast. The shortest retardation time, which can be revealed by indentation test, τ_1, is comparable with the duration of load increase, t_R. Very fast processes (compared to t_R) cannot be revealed, and their parameters are hidden in the "time-independent" compliance constant C_0. Fortunately, the detailed knowledge of response during the first instants of loading is often not necessary.

6. Further information on viscoelastic response from indentation tests

Indentation testing can give also other useful information, for example about apparent modulus and hardness, or relative importance of individual deformation processes.

6.1. *Apparent modulus* E(t)

Deformation of a viscoelastic body under monotonic load is directly proportional to the creep compliance function and indirectly proportional to the apparent reduced modulus, so that

$$E_r(t) = 1/J(t) \tag{25}$$

the uniaxial apparent modulus $E(t)$ is obtained from E_r via Eq. (5). The Poisson's ratio ν is often assumed constant. For very compliant viscoelastic materials, incompressibility ($\nu = 0.5$) may be assumed; for solid polymers usually $\nu < 0.5$.

Caution is necessary if irreversible deformations occurred during the test, as they are implicitly contained in $J(t)$.

6.2. Apparent hardness H(t)

Hardness, defined as the mean contact pressure under load, characterizes the resistance against penetration by another body. In viscoelastic materials it decreases with time as

$$H(t) = F/A(t) \tag{26}$$

For a pointed indenter, $A(t) = kh_c^2(t)$. Cheng and Cheng [28] have shown by finite-element modeling that the ratio of contact depth to the depth of indenter penetration into viscoelastic materials is constant, independent of the rate or duration of loading, $h_c/h = \text{const}$. For a pointed indenter, $h^2(t) \sim J(t)$, so that $H(t) \sim F/J(t)$. Thus, if the "hardness" $H(t')$ from a load-unload test with a characteristic time t' is known, the mean contact pressure $H(t)$, corresponding to another time t under load, can be calculated as

$$H(t) = H(t')J(t')/J(t) \tag{27}$$

where $J(t')$ is the value of creep compliance function corresponding to t'. A similar approach was used by Oyen [16].

6.3. Importance of various deformation processes

The simplest characteristic is the ratio $J(0)/J(t)$ or $J(0)/J(\infty)$, showing what part of the total compliance is instantaneous. The reciprocal, $J(\infty)/J(0)$, can be used for the estimation of maximum possible deformation. These non-dimensional quantities enable the comparison of response of various materials. Also, other characteristics can be defined. The elements in a spring and dashpot model correspond to various processes in the material (with retardation times τ_1, τ_2…), although these relations can be rather loose. The constants C_0, C_1… in the creep compliance function reflect the significance of these processes and together they form the retardation (relaxation) spectrum. The quantities C_1/C_0, C_2/C_0… or $C_0/C\infty$, $C_1/C\infty$ … express the relative proportions of individual processes.

7. Conclusions

Load response of polymeric materials may be characterized by a creep compliance function, whose parameters can be obtained from the time course of indenter penetration. The paper has presented formulae and a procedure for the preparation and evaluation of such tests, and analyzed the results obtained by experiments. The parameters in a creep function have no rigorous physical meaning and should be understood as regression constants of a particular model rather than genuine material characteristics. The arrangement of tests (indenter shape, creep compliance function and test duration) must be chosen with respect to the purpose of measurement. High stresses under a pointed indenter cause irreversible plastic and viscous deformations. If only low stresses are expected in applications, spherical indenters and low loads are better. The test duration and number of elements in a model should be adjusted to the times common in applications or to the duration of delayed processes.

Acknowledgment

The work was supported by the Grant Agency of Czech Republic (projects GAČR 103/08/1340, GAČR 103/08/1197 and GAČR 103/09/1748).

References

[1] W.C. Oliver, G.M. Pharr, An improved technique for determining hardness and elastic modulus using load and displacement sensing indentation experiments, J. Mater. Res. 7 (1992) 1564–1583.
[2] A.C. Fischer-Cripps, Nanoindentation. Springer, New York, 2002.
[3] ISO 14577 Metallic Materials – Instrumented Indentation Test for Hardness and Materials Parameters. Part 1: Test Method. International Organization for Standardization, 2002.
[4] A. Strojny, W.W. Gerberich, Experimental analysis of viscoelastic behavior in nanoindentation. In [6], 159–164.
[5] L. Cheng, L.E. Scriven, W.W. Gerberich, Viscoelastic analysis of micro- and nanoindentation. In [6], 193–198.
[6] N.R. Moody, W.W. Gerberich, N. Burnham, S.P. Baker, Fundamentals of nanoindentation and Nanotribology, Mat. Res. Soc. Symp. Proc. Vol. 522 (1998) MRS, Warrendale, Pennsylvania.
[7] S. Shimizu, T. Yanagimoto, M. Sakai, The pyramidal indentation load-depth curve of viscoelastic materials, J. Mater. Res. 14 (1999) 4075–4086.
[8] S. Lee, W.G. Knauss, A note on the determination of relaxation and creep data from ramp tests, Mechanics Time-Dependent Mater. 4 (2000) 1–7.
[9] L. Cheng, X. Xia, W. Yu, L.E. Scriven, W.W. Gerberich, Flat-punch indentation of a viscoelastic material, J. Polym. Sci. B. Polym. Phys. 38 (2000) 10–22.
[10] H. Lu, B. Wang, J. Ma, G. Huang, H. Wiswanathan, Measurement of creep compliance of solid polymers by nanoindentation, Mechanics Time-Dependent Mater. 7 (2003) 189–207.
[11] S. Yang, Y.W. Zhang, K.A. Zeng, Analysis of nanoindentation creep for polymeric materials, J. Appl. Phys. 95 (2004) 3655–3666.
[12] C.Y. Zhang, Y.W. Zhang, K.Y. Zeng, L. Shen, Nanoindentation of polymers with a sharp indenter, J. Mater. Res. 20 (2005) 1597–1605.
[13] L. Cheng, X. Xia, L.E. Scriven, W.W. Gerberich, Spherical-tip indentation of viscoelastic material, Mechanics Mater. 37 (2005) 213–226.
[14] M.L. Oyen, R.F. Cook, Load-displacement behavior during sharp indentation of viscous-elastic-plastic materials, J. Mater. Res. 18 (2003) 139–149.
[15] M.L. Oyen, Spherical indentation creep following ramp loading, J. Mater. Res. 20 (2005) 2094–2100.
[16] M.L. Oyen, Analytical techniques for indentation of viscoelastic materials, Phil. Mag 86 (2006) 5625–5641.
[17] G.M. Odegard, T.S. Gates, H.M. Herring, Characterization of viscoelastic properties of polymeric materials through nanoindentation, Exper. Mech. 45 (2005) 130–136.
[18] C.A. Tweedie, K.J. Van-Vliet, Contact creep compliance of viscoelastic materials via nanoindentation, J. Mater. Res. 21 (2006) 1576–1589.
[19] S.N. Dub, M.L. Trunov, Determination of viscoelastic material parameters by step-loading nanoindentation, J. Phys. D: Appl. Phys. 41 (2008) 1–6.
[20] J. Lukeš, J. Němeček, J. Minster, Measurement of viscoelastic properties of thermosetting material using nanoindentation. Proc. 25th Danubia-Adria Symposium on Advances in Experimental Mechanics. České Budějovice, 24-27.9.2008. ČVUT Prague, 2008. pp. 161–162.
[21] J. Menčík, L.H. He, M.V. Swain, Determination of viscoelastic-plastic material parameters of biomaterials by instrumented indentation, J. Mech. Behav. Biomed. 2 (2009) 318–325.
[22] J. Menčík, Determination of parameters of viscoelastic materials by instrumented indentation. Part 3: rheological model and other chracteristics, Chem. Listy 104 (2010) s275–s278 (special issue No. 15, ISSN 1213-7103, 0009-2770 printed).
[23] Y.A. Yee, M. Lee, Comparative analysis on the nanoindentation of polymers using atomic force microscopy, Polym. Test. 29 (2010) 95–99.
[24] J. Menčík, L. Beneš, Determination of viscoelastic properties by nanoindentation, J. Optoel. Adv. Mater. 10 (2008) 3288–3291.
[25] E.H. Lee, J.R.M. Radok, The contact problem for viscoelastic bodies, Trans. ASME, Ser. E, J. Appl. Mechanics 27 (1960) 438–444.

[26] K.L. Johnson, Contact Mechanics. Cambridge University Press, Cambridge, 1985.
[27] Y.M. Haddad, Viscoelasticity of Engineering Materials. Chapman & Hall, London, 1995.
[28] Y.T. Cheng, C.M. Cheng, Relationships between initial unloading slope, contact depth, and mechanical properties for conical indentation in linear viscoelastic solids, J. Mater. Res. 20 (2005) 1046–1053.
[29] G. Huang, B. Wang, H. Lu, Measurements of viscoelastic functions of polymers in the frequency-domain using nanoindentation, Mech. Time-dependent. Mater. 8 (2004) 345–364.
[30] E.G. Herbert, W.C. Oliver, G.M. Pharr, Nanoindentation and the dynamic characterization of viscoelastic solids, J. Phys. D: Appl. Phys. 41 (2008) 1–9.
[31] J. Menčík, G. Rauchs, J. Bardon, A. Riche, Determination of elastic modulus and hardness of viscoelastic-plastic materials by instrumented indentation under harmonic load, J. Mater. Res. 20 (2005) 2660–2669.
[32] J. Němeček, Creep effects in nanoindentation of hydrated phases of cement pastes, Mater. Charact 60 (2009) 1028–1034.
[33] T. Chudoba, F. Richter, Investigation of creep behaviour under load during indentation experiments and its influence on hardness and modulus results, Surf. Coat. Technol. 148 (2001) 191–198.
[34] G. Feng, A.H.W. Ngan, Effects of creep and thermal drift on modulus measurement using depth-sensing indentation, J. Mater. Res. 17 (2002) 660–668.